Attention-Based Recurrency for Multi-Agent Reinforcement Learning under State Uncertainty

Thomy Phan
LMU Munich
thomy.phan@ifi.lmu.de

Fabian Ritz
LMU Munich

Jonas Nüßlein
LMU Munich

Michael Kölle
LMU Munich

Thomas Gabor
LMU Munich

Claudia Linnhoff-Popien
LMU Munich

ABSTRACT

State uncertainty poses a major challenge for decentralized coordination, where multiple agents act according to noisy observations without any access to other agents' information. *Centralized training for decentralized execution (CTDE)* is a multi-agent reinforcement learning paradigm, which exploits global information to learn a centralized value function in order to derive coordinated multi-agent policies. State-based CTDE has become popular in multi-agent research due to remarkable progress in the *StarCraft Multi-Agent Challenge (SMAC)*. However, SMAC scenarios are less suited for evaluation against state uncertainty due to deterministic observations and low variance in initial states. Furthermore, state-based CTDE largely neglects state uncertainty w.r.t. decentralization of agents and observations thus being possibly less effective in more general settings. In this paper, we address state uncertainty and introduce *MessySMAC*, a modified version of SMAC with stochastic observations and higher variance in initial states to provide a more general and configurable benchmark. We then propose *Attention-based Embeddings of Recurrency In multi-Agent Learning (AERIAL)* to approximate value functions under consideration of state uncertainty. AERIAL replaces the true state in CTDE with the memory representation of all agents' recurrent functions, which are processed by a self-attention mechanism. We evaluate AERIAL in Dec-Tiger as well as in a variety of SMAC and MessySMAC maps, and compare the results with state-based CTDE. We also evaluate the robustness of AERIAL and state-based CTDE against various configurations of state uncertainty in MessySMAC.

KEYWORDS

Dec-POMDP, State Uncertainty, Multi-Agent Learning, Recurrency, Self-Attention

1 INTRODUCTION

A wide range of potential real-world applications like fleet management, industry 4.0 scenarios, or communication networks, can be formulated as *decentralized partially observable Markov decision process (Dec-POMDP)* representing a cooperative *multi-agent system (MAS)*, where agents have to coordinate in a decentralized way to achieve a common goal [9, 17, 22, 24]. *State uncertainty* poses a major challenge for decentralized coordination in Dec-POMDPs due to noisy sensors and potentially high variance in initial states which are common in the real world [16, 22, 23].

Multi-agent reinforcement learning (MARL) is a general approach to tackle Dec-POMDPs with remarkable progress in recent years [27, 29, 30, 35]. Current state-of-the-art MARL uses *centralized training for decentralized execution (CTDE)*, where training takes place in a laboratory or a simulator with access to global information [9, 18, 27]. For example, *state-based CTDE* exploits true state information to learn a centralized value function in order to derive coordinated policies for decentralized decision making [9, 24, 27]. Due to its empirical success in the *StarCraft Multi-Agent Challenge (SMAC)*, state-based CTDE has become popular in MARL research and is widely assumed to be an adequate approach to general Dec-POMDPs [9, 19, 20].

However, merely relying on SMAC and state-based CTDE can be a pitfall in practice as state uncertainty is largely neglected – despite being an important aspect in Dec-POMDPs [19, 22, 23]:

- SMAC provides a rich set of multi-agent challenges but the scenarios exhibit very limited state uncertainty due to deterministic observations and low variance in initial states [7]. Therefore, SMAC scenarios only represent simplified special cases rather than general Dec-POMDP challenges [19].
- Purely state-based value functions are insufficient to evaluate and adapt multi-agent behavior, since all agents make decisions on a completely different basis, i.e., individual histories of noisy observations and actions. True Dec-POMDP value functions consider state uncertainty w.r.t. decentralization of agents and observations though [23].
- The optimal state-based value function represents an upper-bound of the true optimal Dec-POMDP value function thus purely state-based CTDE can result in overly optimistic behavior in general Dec-POMDPs [19, 25].

Recent works investigated potential weaknesses of state-based CTDE for multi-agent actor-critic methods [19, 20]. The experimental results show that state-based CTDE can surprisingly fail in very simple Dec-POMDP benchmarks that exhibit higher degrees of state uncertainty than SMAC. While these studies can be considered an important step towards general Dec-POMDPs, there is neither an approach which actually considers state uncertainty nor a benchmark to systematically evaluate such an approach yet.

In this paper, we introduce *MessySMAC*, a modified version of SMAC with stochastic observations and higher variance in initial states to provide a more general and configurable Dec-POMDP benchmark. We then propose *Attention-based Embeddings of Recurrency In multi-Agent Learning (AERIAL)* to approximate value functions under consideration of state uncertainty. AERIAL replaces the true state in CTDE with the memory representation of all agents' recurrent functions, which are processed by a self-attention mechanism. Our contributions are as follows:

- We introduce MessySMAC to enable systematic evaluation under different configurations of state uncertainty.
- We formulate AERIAL and explain how the concepts better fit in the general Dec-POMDP setting than state-based CTDE.
- We evaluate AERIAL in Dec-Tiger, a small and traditional Dec-POMDP benchmark, as well as in a variety of SMAC and MessySMAC maps, and compare the results with state-based CTDE. Our results show that AERIAL achieves competitive performance in SMAC, and superior performance in Dec-Tiger and MessySMAC. We also evaluate the robustness of AERIAL and state-based CTDE against various configurations of state uncertainty in MessySMAC.

2 BACKGROUND

2.1 Decentralized POMDPs

We formulate cooperative MAS problems as *Dec-POMDP* $M = \langle \mathcal{D}, \mathcal{S}, \mathcal{A}, \mathcal{T}, \mathcal{R}, \mathcal{Z}, \Omega, b_0 \rangle$, where $\mathcal{D} = \{1, ..., N\}$ is a set of agents i, $\mathcal{S}$ is a set of (true) states s_t at time step t, $\mathcal{A} = \langle \mathcal{A}_i \rangle_{i \in \mathcal{D}}$ is the set of joint actions $\mathbf{a_t} = \langle a_{t,1}, ..., a_{t,N} \rangle = \langle a_{t,i} \rangle_{i \in \mathcal{D}}$, $\mathcal{T}(s_{t+1}|s_t, \mathbf{a_t})$ is the state transition probability, $r_t = \mathcal{R}(s_t, \mathbf{a_t}) \in \mathbb{R}$ is the shared reward, $\mathcal{Z}$ is a set of local observations $z_{t,i}$ for each agent $i \in \mathcal{D}$, $\Omega(\mathbf{z_{t+1}}|\mathbf{a_t}, s_{t+1})$ is the probability of joint observation $\mathbf{z_{t+1}} = \langle z_{t+1,i} \rangle_{i \in \mathcal{D}} \in \mathcal{Z}^N$, and b_0 is the probability distribution over initial states s_0 [22, 23]. Each agent i maintains a *local history* $\tau_{t,i} \in (\mathcal{Z} \times \mathcal{A}_i)^t$ and $\boldsymbol{\tau_t} = \langle \tau_{t,i} \rangle_{i \in \mathcal{D}}$ is the *joint history*. A *belief state* $b(s_t|\boldsymbol{\tau_t})$ is a sufficient statistic for joint history $\boldsymbol{\tau_t}$ and defines a probability distribution over true states s_t which can be updated by Bayes' theorem [16, 22]. Joint quantities are written in bold face.

A *joint policy* $\boldsymbol{\pi} = \langle \pi_i \rangle_{i \in \mathcal{D}}$ with *decentralized* or *local policies* π_i defines a deterministic mapping from joint histories to joint actions $\boldsymbol{\pi}(\boldsymbol{\tau_t}) = \langle \pi_i(\tau_{t,i}) \rangle_{i \in \mathcal{D}} \in \mathcal{A}$. The *return* is defined by $G_t = \sum_{c=0}^{T-1} \gamma^c r_{t+c}$, where T is the *horizon* and $\gamma \in [0, 1]$ is the *discount factor*. $\boldsymbol{\pi}$ can be evaluated with a *value function* $Q^{\boldsymbol{\pi}}(\boldsymbol{\tau_t}, \mathbf{a_t}) = \mathbb{E}_{b_0, \mathcal{T}, \Omega}[G_t | \boldsymbol{\tau_t}, \mathbf{a_t}, \boldsymbol{\pi}]$. The goal is to find an *optimal joint policy* $\boldsymbol{\pi}^*$ with *optimal value function* $Q^{\boldsymbol{\pi}^*} = Q^*$ as defined in the next section.

2.2 Optimal Value Functions and Policies

Fully observable MAS. In MDP-like settings with a centralized controller, the optimal value function Q^*_{MDP} is defined by [3, 36]:

$$Q^*_{MDP}(s_t, \mathbf{a_t}) = r_t + \gamma \sum_{s_{t+1} \in \mathcal{S}} \mathcal{T}(\cdot) max_{\mathbf{a_{t+1}} \in \mathcal{A}} Q^*_{MDP}(s_{t+1}, \mathbf{a_{t+1}}) \quad (1)$$

where $\mathcal{T}(\cdot) = \mathcal{T}(s_{t+1}|s_t, \mathbf{a_t})$.

Due to the Markov property and full observability of true states, Q^*_{MDP} does not depend on $\boldsymbol{\tau_t}$ but on s_t. Thus, decentralized observations $z_{t,i}$ and probabilities according to Ω and b_0 do not need to be considered at all. An optimal (joint) policy $\boldsymbol{\pi}^*_{\mathbf{MDP}}$ of the centralized controller simply maximizes Q^*_{MDP} for all true states s_t [23, 36]:

$$\boldsymbol{\pi}^*_{\mathbf{MDP}} = argmax_{\boldsymbol{\pi}_{\mathbf{MDP}}} \sum_{s_t \in \mathcal{S}} Q^*_{MDP}(s_t, \boldsymbol{\pi}_{\mathbf{MDP}}(s_t)) \quad (2)$$

Partially observable MAS. In general Dec-POMDPs, where true states are not observable and only decentralized controllers or agents exist, the optimal value function Q^* is defined by [23]:

$$Q^*(\boldsymbol{\tau_t}, \mathbf{a_t}) = \sum_{s_t \in \mathcal{S}} b(s_t|\boldsymbol{\tau_t}) \left(r_t + \gamma \sum_{s_{t+1} \in \mathcal{S}} \sum_{\mathbf{z_{t+1}} \in \mathcal{Z}^N} \mathcal{T}(\cdot) \Omega(\cdot) Q^*(\cdot) \right) \quad (3)$$

where $\mathcal{T}(\cdot) = \mathcal{T}(s_{t+1}|s_t, \mathbf{a_t})$, $\Omega(\cdot) = \Omega(\mathbf{z_{t+1}}|\mathbf{a_t}, s_{t+1})$, $Q^*(\cdot) = Q^*(\boldsymbol{\tau_{t+1}}, \boldsymbol{\pi}^*(\boldsymbol{\tau_{t+1}}))$, and $\boldsymbol{\tau_{t+1}}$, is the concatenation of $\boldsymbol{\tau_t}$, $\mathbf{a_t}$, and $\mathbf{z_{t+1}}$.

An optimal joint policy $\boldsymbol{\pi}^*$ for decentralized execution maximizes the expectation of Q^* for all joint histories $\boldsymbol{\tau_t}$ [8, 23]:

$$\boldsymbol{\pi}^* = argmax_{\boldsymbol{\pi}} \sum_{t=0}^{T-1} \sum_{\boldsymbol{\tau_t} \in (\mathcal{Z}^N \times \mathcal{A})^t} C(\boldsymbol{\tau_t}, \boldsymbol{\pi}) \mathbf{P}(\boldsymbol{\tau_t}|\boldsymbol{\pi}, b_0) Q^*(\boldsymbol{\tau_t}, \boldsymbol{\pi}(\boldsymbol{\tau_t})) \quad (4)$$

where the indicator $C(\boldsymbol{\tau_t}, \boldsymbol{\pi})$ filters out joint histories $\boldsymbol{\tau_t}$ that are inconsistent with $\boldsymbol{\pi}$ and probability $\mathbf{P}(\boldsymbol{\tau_t}|\boldsymbol{\pi}, b_0)$ considers state uncertainty w.r.t. decentralization of agents and observations [23]:

$$\begin{aligned} \mathbf{P}(\boldsymbol{\tau_t}|\boldsymbol{\pi}, b_0) &= \mathbf{P}(\mathbf{z_0}|b_0) \prod_{c=1}^{t} \mathbf{P}(\mathbf{z_c}|\boldsymbol{\tau_{c-1}}, \boldsymbol{\pi}) \\ &= \mathbf{P}(\mathbf{z_0}|b_0) \prod_{c=1}^{t} \sum_{s_c \in \mathcal{S}} \sum_{s_{c-1} \in \mathcal{S}} \mathcal{T}(\cdot) \Omega(\cdot) \end{aligned} \quad (5)$$

where $\mathcal{T}(\cdot) = \mathcal{T}(s_c|s_{c-1}, \boldsymbol{\pi}(\boldsymbol{\tau_{c-1}}))$ and $\Omega(\cdot) = \Omega(\mathbf{z_c}|\boldsymbol{\pi}(\boldsymbol{\tau_{c-1}}), s_c)$.

Since all agents act independently based on their local history $\tau_{t,i}$ without knowing the complete joint history $\boldsymbol{\tau_t}$, the probability $\mathbf{P}(\boldsymbol{\tau_t}|\boldsymbol{\pi}, b_0)$ depends on all previous observations, actions, and the respective probabilities according to b_0, $\mathcal{T}$, and Ω [23].

Q^*_{MDP} is proven to represent an upper bound of Q^* [23]. Thus, naively deriving local policies π_i from Q^*_{MDP} instead of Q^* can result in overly optimistic behavior as shown in Section 5.1 and 6.

2.3 Multi-Agent Reinforcement Learning

Finding an optimal joint policy $\boldsymbol{\pi}^*$ via exhaustive computation of Q^* according to Eq. 3-5 is intractable in practice [21, 22, 31]. MARL offers a scalable way to learn Q^* and $\boldsymbol{\pi}^*$ via function approximation, e.g., using CTDE, where training takes place in a laboratory or a simulator with access to global information [9, 18, 27]. We focus on value-based MARL to learn a centralized value function $Q_{tot} \approx Q^*$, which can be factorized into *local value functions* $\langle Q_i \rangle_{i \in \mathcal{D}}$ for decentralized decision making via $\pi_i(\tau_{t,i}) = argmax_{a_{t,i} \in \mathcal{A}_i} Q_i(\tau_{t,i}, a_{t,i})$. For that, a *factorization operator* Ψ is used [24, 26]:

$$Q_{tot}(\boldsymbol{\tau_t}, \mathbf{a_t}) = \Psi(Q_1(\tau_{t,1}, a_{t,1}), ..., Q_N(\tau_{t,N}, a_{t,N})) \quad (6)$$

In practice, Ψ is realized with deep neural networks, such that $\langle Q_i \rangle_{i \in \mathcal{D}}$ can be learned end-to-end via backpropagation by minimizing the mean squared *temporal difference (TD)* error [27, 29, 30]. A factorization operator Ψ is *decentralizable* when satisfying the *IGM (Individual-Global-Max)* such that [29]:

$$argmax_{\mathbf{a_t} \in \mathcal{A}} Q_{tot}(\boldsymbol{\tau_t}, \mathbf{a_t}) = \begin{pmatrix} argmax_{a_{t,1} \in \mathcal{A}_1} Q_1(\tau_{t,1}, a_{t,1}) \\ ... \\ argmax_{a_{t,N} \in \mathcal{A}_N} Q_N(\tau_{t,N}, a_{t,N}) \end{pmatrix} \quad (7)$$

There exists a variety of factorization operators Ψ, which satisfy Eq. 7 using monotonic constraints like QMIX [27, 30], nonlinear transformation like QPLEX [29, 35], or loss weighting like CW- and OW-QMIX [25]. Most factorization approaches use state-based

CTDE, where true states s_t are additionally integrated in Ψ to approximate Q^*_{MDP} according to Eq. 1 instead of Q^* [25, 27, 35].

2.4 Recurrent Reinforcement Learning

In partially observable settings, the policy π_i of agent i conditions on the history $\tau_{t,i}$ of past observations and actions [16, 22]. In practice, *recurrent neural networks (RNNs)* like LSTMs or GRUs are used to learn a compact representation $h_{t,i}$ of $\tau_{t,i}$ and π_i known as *hidden state* or *memory representation*[1], which implicitly encodes the *recurrency* of agent i, i.e., the distribution P_i over $\tau_{t,i}$ [6, 12, 13]:

$$P_i(\tau_{t,i}|\pi_i, b_0) = P_i(z_{0,i}|b_0) \prod_{c=1}^{t} P_i(z_{c,i}|\tau_{c-1,i}, \pi_i(\tau_{c-1,i})) \quad (8)$$

RNNs are commonly used for partially observable problems and have been empirically shown to be more effective than using raw observations $z_{t,i}$ or histories $\tau_{t,i}$ [9, 11, 28, 34].

3 RELATED WORK

Multi-Agent Reinforcement Learning. In recent years, MARL has achieved remarkable progress in challenging domains [4, 10, 32, 34]. Current state-of-the-art MARL uses CTDE to learn a centralized value function Q_{tot} for actor-critic learning [9, 18] or factorization [25, 27, 29, 30, 35]. However, the majority of works assumes a simplified Dec-POMDP setting, where Ω is deterministic, and uses state-based CTDE to approximate Q^*_{MDP} according to Eq. 1 instead of Q^*. State-based CTDE largely neglects state uncertainty thus being possibly less effective in more general Dec-POMDP settings. We propose an approach to *implicitly consider* state uncertainty by exploiting the *recurrency of all agents* using *self-attention* in CTDE instead of relying on true states.

Weaknesses of State-Based CTDE. Recent works investigated potential weaknesses of state-based CTDE for multi-agent actor-critic methods regarding bias and variance [19, 20]. The experimental results show that state-based CTDE can surprisingly fail in very simple Dec-POMDP benchmarks that exhibit higher degrees of state uncertainty than SMAC. While these studies can be considered an important step towards general Dec-POMDPs, there is neither an approach which actually considers state uncertainty nor a benchmark to systematically evaluate such an approach yet. In this work, we focus on *value-based MARL*, where learning an accurate value function is important for meaningful factorization, and propose an *attention-based recurrency approach* to value function approximation under consideration of state uncertainty. We also introduce a *modified* SMAC benchmark, which enables systematic evaluation under different configurations of state uncertainty.

Attention-Based CTDE. Attention has been used in CTDE to process information of potentially variable length N, where joint observations $\mathbf{z_t}$, joint actions $\mathbf{a_t}$, or local values $\langle Q_i \rangle_{i \in \mathcal{D}}$ are weighted and aggregated to provide a meaningful representation for value function approximation [14, 15, 35, 37, 38]. Most works focus on Markov games, where joint observations are deterministic or even Markovian, which does not apply to general Dec-POMDP settings. In this work, we address *state uncertainty in Dec-POMDPs* and propose a CTDE approach, where self-attention is applied to the *memory representations* $h_{t,i}$ of all agents' RNNs instead of raw observations $z_{t,i}$. Since $h_{t,i}$ encodes the individual distribution P_i over local histories $\tau_{t,i}$ (Eq. 8), our approach implicitly considers state uncertainty w.r.t. decentralization of agents and observations to approximate the *true optimal value function* Q^* (Eq. 3-5).

[1] In this paper, we use the term *memory representation* to avoid confusion with the state terminology of the (Dec-)POMDP literature [16, 22].

4 A GENERAL DEC-POMDP BENCHMARK WITH HIGH STATE UNCERTAINTY

4.1 Motivation

StarCraft Multi-Agent Challenge (SMAC) provides a rich set of micromanagement tasks, where a team of learning agents has to fight against an enemy team, which acts according to handcrafted heuristics of the built-in StarCraft AI [28]. SMAC currently represents the de facto standard for MARL evaluation regarding decentralized coordination and multi-agent credit assignment [9, 25, 27, 35]. However, SMAC scenarios exhibit very limited state uncertainty due to deterministic observations and low variance in initial states therefore only representing simplified special cases rather than general Dec-POMDP challenges [7, 19]. To assess practical applicability of MARL, we need benchmarks with sufficiently high degrees of state uncertainty as real-world problems are generally messy and only observable through noisy sensors [16, 22, 23].

4.2 MessySMAC

MessySMAC is a modified version of SMAC with stochastic observation functions Ω, where the observation values are negated with a probability of $\phi \in [0, 1)$. To increase variance in initial states w.r.t. b_0, we initially perform K random steps before officially starting an episode. MessySMAC represents a more general Dec-POMDP challenge which enables systematic evaluation under different configurations of state uncertainty according to ϕ and K.

Fig. 1 shows the PCA visualization of (deterministic) joint observations in the maps `10m_vs_11m` and `3s_vs_5z` in SMAC ($K = 0$) and in MessySMAC ($K = 10$) within the first 5 steps of 1,000 episodes using a random policy. While the observations of the initial state s_0 (dark purple) in original SMAC are very similar and can be easily distinguished from subsequent steps, the separability in MessySMAC is much harder, indicating higher state uncertainty due to significantly higher entropy in b_0. The impact of ϕ and K on state-of-the-art MARL is systematically evaluated in Section 6.4.

4.3 Comparison with SMACv2

SMACv2 is an update to the original SMAC benchmark featuring random initial positions and unit types as well as further restrictions w.r.t. agent observations, which was developed in parallel to our work [7]. SMACv2 addresses similar issues as MessySMAC but MessySMAC additionally features *stochastic observations* w.r.t. Ω according to the general Dec-POMDP formulation in Section 2.1. Unlike MessySMAC, SMACv2 does not support the *original SMAC maps* which makes direct comparison under different configurations of state uncertainty difficult.

Therefore, SMACv2 can be regarded as entirely new StarCraft II benchmark with more stochasticity, while MessySMAC represents a *SMAC extension*, enabling systematic evaluation under different configurations of state uncertainty for the original SMAC maps.

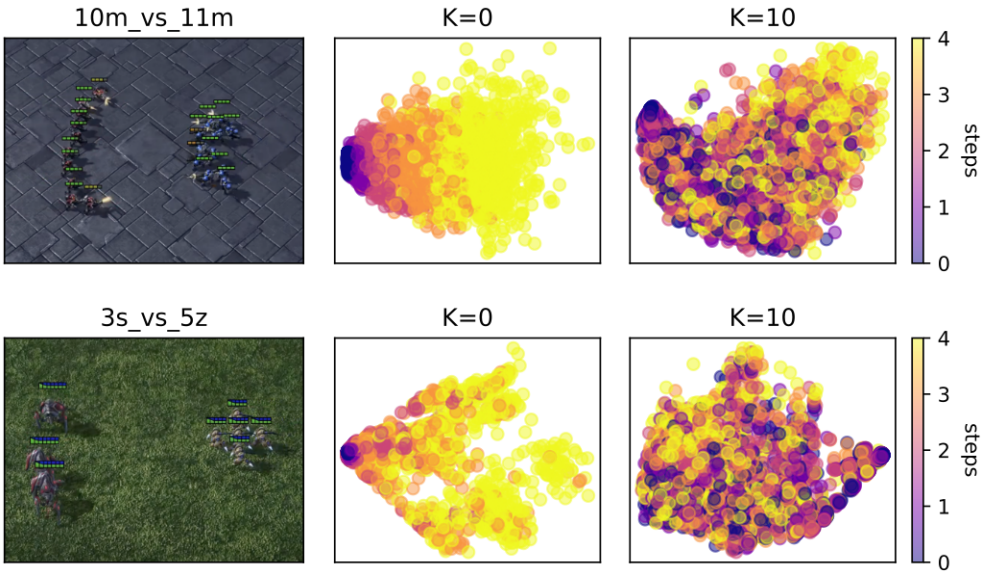

Figure 1: *Left:* Screenshot of two SMAC maps. *Middle:* PCA visualization of the joint observations in original SMAC within the first 5 steps of 1,000 episodes using a random policy (with $K = 0$ initial random steps). *Right:* Analogous PCA visualization for MessySMAC (with $K = 10$ initial random steps). For visual comparability, the observation functions are deterministic here.

5 MARL UNDER STATE UNCERTAINTY

5.1 Motivation

The majority of state-of-the-art works assumes a simplified Dec-POMDP setting, where Ω is deterministic, and approximates Q^*_{MDP} according to Eq. 1 instead of Q^* [9, 25, 27, 28, 35].

If there are only deterministic observations and initial states s_0 such that $b_0(s_0) = 1$ and $b_0(s') = 0$ if $s' \neq s_0$, then $\mathbf{P}(\boldsymbol{\tau_t}|\boldsymbol{\pi}, b_0)$ would only depend on state transition probabilities $\mathcal{T}(s_{t+1}|s_t, \mathbf{a_t})$ which are purely state-based, ignoring decentralization of agents and observations [23]. In such scenarios, state uncertainty is very limited given that all policies π_i are deterministic. We hypothesize this to be one reason why state-based CTDE performs so well in SMAC, since SMAC scenarios have these simplifying properties according to Section 4, Fig. 1, and [7, 19].

In the following, we regard a small Dec-POMDP example with high state uncertainty, where state-based CTDE can fail at finding an optimal joint policy $\boldsymbol{\pi}^*$ according to Eq. 4.

Example. *Dec-Tiger* is a simple and traditional Dec-POMDP benchmark with $N = 2$ agents facing two doors [21]. A tiger is randomly placed behind the left (s_L) or right door (s_R) representing the true state. Both agents are able to listen (li) and open the left (o_L) or right door (o_R). The listening action li produces a noisy observation of either hearing the tiger to be left (z_L) or right (z_R), correctly indicating the tiger's position with 85% chance and a cost of -1 per listening agent. If both agents open the same door, the episode terminates with a reward of -50 if opening the tiger door and +20 otherwise. If both agents open different doors, the episode ends with -100 reward and if only one agent opens a door while the other agent is listening, the episode terminates with -101 if opening the tiger door and +9 otherwise.

Given a horizon of $T = 2$, the tiger being behind the right door (s_R), and both agents having listened in the first step, where agent 1 heard z_L and agent 2 heard z_R: Assuming that both agents learned to perform the same actions, e.g., due to CTDE and parameter sharing [10, 32, 39], Q^*_{MDP} and Q^* would estimate the following values[2]:

$$Q^*_{MDP}(s_R, \langle li, li\rangle) = -2 \qquad Q^*(\boldsymbol{\tau_t}, \langle li, li\rangle) = -2$$
$$Q^*_{MDP}(s_R, \langle o_L, o_L\rangle) = 20 \qquad Q^*(\boldsymbol{\tau_t}, \langle o_L, o_L\rangle) = -15$$
$$Q^*_{MDP}(s_R, \langle o_R, o_R\rangle) = -50 \qquad Q^*(\boldsymbol{\tau_t}, \langle o_R, o_R\rangle) = -15$$

Any policy $\boldsymbol{\pi}^*_{\mathbf{MDP}}$ or decentralizable joint policy $\boldsymbol{\pi}$ w.r.t. IGM (Eq. 7) that maximizes Q^*_{MDP} according to Eq. 2 would optimistically recommend $\langle o_L, o_L\rangle$ based on the true state s_R, regardless of what the agents observed. In practice, this would only be useful if the true state was observable or if the observation function Ω was deterministic as assumed in prior works [25, 27–29]. However, any joint policy $\boldsymbol{\pi}^*$ that maximizes the expectation of Q^* according to Eq. 4 would actually consider state uncertainty w.r.t. decentralization of agents and observations, and recommend $\langle li, li\rangle$ which corresponds to the true optimal decision for $T = 2$ [31]. In Section 6.1, we empirically confirm this example for several state-of-the-art approaches, which approximate Q^*_{MDP} instead of Q^* [25, 27, 35].

5.2 Attention-Based Embeddings of Recurrency

Preliminaries. We now introduce *Attention-based Embeddings of Recurrency In multi-Agent Learning (AERIAL)* to approximate optimal Dec-POMDP value functions Q^* according to Eq. 3-5. Our setup is based on prior factorization approaches, where a factorization

[2]The exact calculation of these values is provided in the appendix A.1

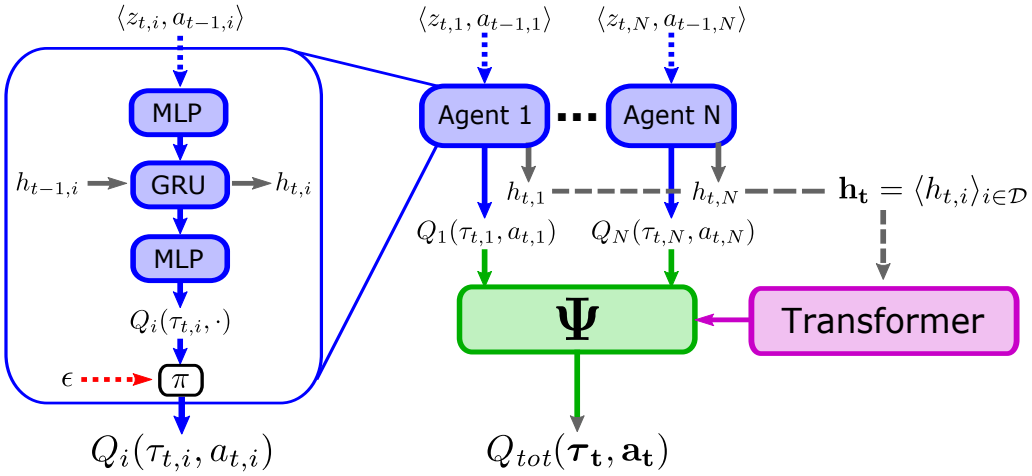

Figure 2: Illustration of the AERIAL setup. *Left:* Recurrent agent network structure. *Right:* Value function factorization via factorization operator Ψ using the joint memory representation $\mathbf{h_t} = \langle h_{t,i} \rangle_{i \in \mathcal{D}}$ of all agents' RNNs instead of true states s_t. All memory representations $h_{t,i}$ are detached from the computation graph to avoid additional differentiation (indicated by the dashed gray arrows) and passed through a simplified transformer before being used by Ψ for value function factorization.

operator Ψ according to Eq. 6-7 like QMIX is available [27, 30, 35]. All agents process their local histories $\tau_{t,i}$ via RNNs as motivated in Section 2.4 and schematically shown in Fig. 2 (left).

Unlike Q^*_{MDP}, the true optimal Dec-POMDP value function Q^* considers state uncertainty w.r.t. decentralization of agents and observations through $\mathbf{P}(\boldsymbol{\tau_t}|\boldsymbol{\pi}, b_0)$ as defined in Eq. 5. Simply replacing s_t with $\boldsymbol{\tau_t}$ as suggested in [19] is not sufficient because the resulting value function would assume a centralized controller which has access to the complete joint history $\boldsymbol{\tau_t}$, in contrast to decentralized agents i which can only access their local history $\tau_{t,i}$ [23].

Exploiting Multi-Agent Recurrency. At first we propose to naively exploit the recurrency of all agents by simply replacing the true state s_t in CTDE with the *joint memory representation* $\mathbf{h_t} = \langle h_{t,i} \rangle_{i \in \mathcal{D}}$ of all agents' RNNs. Since each memory representation $h_{t,i}$ encodes the individual distribution P_i of agent i (Eq. 8) over local histories $\tau_{t,i}$, using $\mathbf{h_t}$ instead of true states s_t could help to implicitly consider agent-wise state uncertainty at least.

This approach, which we call `AERIAL (no attention)`, can already be considered a sufficient solution if we assume conditional independence of all P_i such that $\mathbf{P}(\boldsymbol{\tau_t}|\boldsymbol{\pi}, b_0) = \prod_{i=1}^{N} P_i(\tau_{t,i}|\pi_i, b_0)$.

Attention-Based Recurrency. While `AERIAL (no attention)` offers a simple approach to consider state uncertainty in contrast to state-based CTDE, the independence assumption of all individual distributions P_i does not hold in practice due to correlations in observations and actions [1, 2]. Given the Dec-Tiger example above, the probability for being in state s_R is 0.15 and 0.85 from the perspective of agent 1 and 2 respectively [16]. However, the actual probability according to the belief state $b(s_R|\boldsymbol{\tau_t})$ is $0.5 \neq 0.15 \cdot 0.85$, indicating that all P_i are not conditionally independent [22].

Thus, we additionally process $\mathbf{h_t}$ by a simplified *transformer* to automatically learn the latent dependencies of all memory representations $h_{t,i} \in \mathbf{h_t}$ through self-attention [33]. The resulting approach, which we call `AERIAL`, is shown in Fig. 2.

Since no sequential order of agents is assumed, we do not apply positional encoding or masking. The joint memory representation $\mathbf{h_t}$ is simply passed through a *multi-head attention* layer with each attention head output being defined by [33]:

$$att_c(\mathbf{h_t}) = softmax\left(\frac{W_q(\mathbf{h_t})W_k(\mathbf{h_t})^T}{\sqrt{d_{att}}}\right) W_v(\mathbf{h_t}) \tag{9}$$

where W_q, W_k, and W_v are *multi-layer perceptrons (MLP)* with an output dimensionality of d_{att}. All outputs $att_c(\mathbf{h_t})$ are summed and passed through a series of MLP layers before being input to the factorization operator Ψ, replacing the true state s_t.

To avoid additional differentation of $\mathbf{h_t}$ through Ψ, we detach $\mathbf{h_t}$ from the computation graph. Thus, we make sure that $\mathbf{h_t}$ is only learned through agent RNNs.

5.3 Discussion of AERIAL

AERIAL offers a simple way to adapt existing factorization approaches to general Dec-POMDPs by implicitly considering state uncertainty. The true state s_t originally used to train Ψ via CTDE is replaced by the joint memory representation $\mathbf{h_t}$, which encodes all individual distributions P_i over local histories [6, 13]. The rest of the training pipeline remains unchanged which eases adaptation.

However, the naive independence assumption of agent-wise recurrency via $h_{t,i}$ does not hold in practice due to correlations in observations and actions despite the decentralization [1, 2]. Thus, we employ a transformer to learn the latent dependencies of all memory representations $h_{t,i}$ by using self-attention on $\mathbf{h_t}$ (Eq. 9).

AERIAL does not depend on true states therefore requiring less overall information than state-based CTDE, since we assume $\mathbf{h_t}$ to be available in all CTDE setups anyway [9, 25, 27, 35]. Note that AERIAL does not necessarily require RNNs to obtain $\mathbf{h_t}$ as, e.g., hidden layers of MLPs or decision transformers can be used alternatively to approximate $\mathbf{h_t}$ [5, 29].

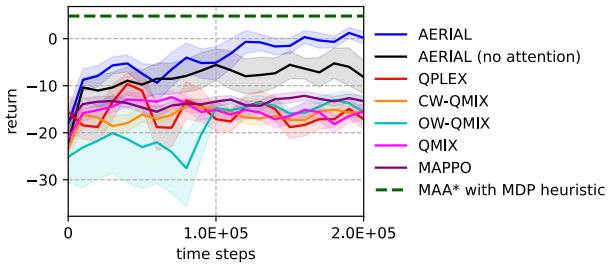

Figure 3: Average learning progress w.r.t. the return of AERIAL variants and state-of-the-art baselines in Dec-Tiger over 50 runs. Shaded areas show the 95% confidence interval.

6 EXPERIMENTS

We use the state-based CTDE implementations of QPLEX, CW-QMIX, OW-QMIX, and QMIX from [25] as state-of-the-art baselines with the same hyperparameters from the paper without further tuning. We also integrate MAPPO with the hyperparameter recommendations from [39].

AERIAL is implemented[3] using QMIX as factorization operator Ψ according to Fig. 2. We also experimented with QPLEX as alternative with no significant difference in performance. Thus, we stick with QMIX for computational efficiency due to less trainable parameters. The transformer of AERIAL has 4 heads with W_q, W_k, and W_v each having one hidden layer of $d_{att} = 64$ units with ReLU activation. The subsequent MLP layers have 64 units with ReLU activation.

For ablation study, we implement AERIAL (no attention), which trains Ψ directly on $\mathbf{h_t}$ without self-attention as described in Section 5.2, and another variant, called AERIAL (raw history), which trains Ψ on the raw joint history $\boldsymbol{\tau_t}$ concatenated with the true state s_t as originally proposed for actor-critic methods [19].

6.1 Dec-Tiger

Setting. We use the Dec-Tiger problem described in Section 5.1 and [21] as simple proof-of-concept domain with $T = 4$ and $\gamma = 1$. We also provide the optimal value of 4.8 computed with MAA* for comparison [31].

Results. The results are shown in Fig. 3. AERIAL comes closest to the optimum, achieving an average return of about zero. AERIAL (no attention) performs second best with an average return of about -8, while all other approaches achieve an average return of about -15.

Discussion. The Dec-Tiger results in Fig. 3 empirically confirm the example from Section 5.1 as well as the findings of [19, 23] that state-based CTDE can struggle in very simple Dec-POMDPs with higher degrees of state uncertainty than SMAC. Most state-based CTDE approaches converge to a one-step policy, where all agents optimistically open the same door as indicated in Section 5.1. In the example, Q^*_{MDP} would estimate a best-case value of 20 for jointly opening a particular door regardless of any agent observation. However, the true value w.r.t. Q^* of jointly opening any door in the beginning is -15, where the tiger would have a 50% chance of being either left or right according to the belief state $b(s_t|\boldsymbol{\tau_t})$. AERIAL (raw history) also fails to find any meaningful policy, indicating that merely using the joint history $\boldsymbol{\tau_t}$ is not sufficient to approximate Q^* as stated in Section 5.2. AERIAL (no attention) converges to a local optimum most of the time, where both agents only listen for all $T = 4$ time steps. AERIAL performs best due to considering the latent dependencies of all memory representations $h_{t,i} \in \mathbf{h_t}$.

[3]Code available at https://github.com/thomyphan/messy_smac

6.2 Original SMAC

Setting. To directly assess the competitiveness of AERIAL against the state-of-the-art baselines, we evaluate in the original SMAC maps 3s5z and 10m_vs_11m which are classified as *easy*, as well as the *hard* maps 2c_vs_64zg, 3s_vs_5z, and 5m_vs_6m, and the *super hard* map 3s5z_vs_3s6z [28].

Results. The average test win rates at the end of training for each SMAC map are shown in Table 1. AERIAL and AERIAL (no attention) achieve competitive performance compared to QPLEX and QMIX in the easy maps 3s5z and 10m_vs_11m, while performing best in 3s_vs_5z, 5m_vs_6m, and 3s5z_vs_3s6z. In the *super hard* scenario, AERIAL, AERIAL (no attention), and MAPPO are the only approaches achieving an average test win rate of more than 15%. However in the hard map 2c_vs_64zg, QMIX, OW-QMIX, and MAPPO outperform AERIAL and AERIAL (no attention). AERIAL (raw history) performs worst in most maps.

Discussion. The results in Table 1 show that AERIAL and AERIAL (no attention) are able to compete with state-of-the-art baselines in the original SMAC benchmark without sacrificing performance when replacing the true state s_t with the joint memory representation $\mathbf{h_t}$ in CTDE. Despite being able to outperform the baselines in hard and super hard maps except 2c_vs_64zg, we do not claim significant outperformance, since we regard most SMAC maps as widely solved by the community [7]. AERIAL (raw history) is unable to find any meaningful policy, possibly due to the high dimensionality of $\boldsymbol{\tau_t}$ and s_t which are harder to process than the more compact yet informative memory representations $h_{t,i} \in \mathbf{h_t}$.

6.3 MessySMAC

Setting. Analogously to SMAC, we evaluate AERIAL in the MessySMAC maps 3s5z, 10m_vs_11m, 2c_vs_64zg, 3s_vs_5z, 5m_vs_6m, and 3s5z_vs_3s6z. We set $\phi = 15\%$ and $K = 10$.

Results. The results for MessySMAC are shown in Fig. 4. AERIAL performs best in all maps with AERIAL (no attention) being second best except in 2c_vs_64zg. In the symmetric map 3s5z and asymmetric map 3s_vs_5z, AERIAL (no attention) performs almost as well as AERIAL. QMIX and QPLEX are the best performing state-of-the-art baselines in most maps. In the super hard map 3s5z_vs_3s6z, only AERIAL and AERIAL (no attention) are able to progress notably. AERIAL (raw history) performs worst in all maps. MAPPO only progresses notably in 2c_vs_64zg.

Discussion. The performance of AERIAL (no attention) indicates that simply replacing the true state s_t with the joint memory representation $\mathbf{h_t}$ can already be beneficial in domains with high state uncertainty w.r.t. Ω and b_0 as hypothesized in Section 5.2.

Table 1: Average win rate of AERIAL variants and state-of-the-art baselines after 2 million time steps of training across 400 final test episodes for the original SMAC maps with the 95% confidence interval. The best results per map are highlighted in boldface and blue.

	AERIAL variants			state-of-the-art baselines				
	AERIAL	no attention	raw history	QPLEX	CW-QMIX	OW-QMIX	QMIX	MAPPO
3s5z	**0.95 ± 0.01**	0.90 ± 0.03	0.18 ± 0.11	0.94 ± 0.01	0.87 ± 0.02	0.91 ± 0.02	**0.95 ± 0.01**	68.7 ± 0.94
10m_vs_11m	**0.97 ± 0.01**	0.88 ± 0.04	0.09 ± 0.14	0.90 ± 0.02	0.91 ± 0.02	0.96 ± 0.01	0.90 ± 0.02	77.3 ± 0.66
2c_vs_64zg	0.52 ± 0.11	0.29 ± 0.14	0.02 ± 0.03	0.29 ± 0.1	0.38 ± 0.12	0.55 ± 0.13	0.59 ± 0.11	**90.2 ± 0.24**
3s_vs_5z	**0.96 ± 0.02**	**0.96 ± 0.02**	0.38 ± 0.13	0.74 ± 0.11	0.18 ± 0.06	0.08 ± 0.04	0.81 ± 0.05	73.8 ± 0.44
5m_vs_6m	**0.77 ± 0.03**	0.71 ± 0.04	0.1 ± 0.11	0.66 ± 0.04	0.41 ± 0.04	0.55 ± 0.06	0.67 ± 0.05	60.6 ± 1.13
3s5z_vs_3s6z	0.18 ± 0.09	**0.21 ± 0.15**	0.0 ± 0.0	0.1 ± 0.03	0.0 ± 0.0	0.02 ± 0.01	0.02 ± 0.02	20.5 ± 2.91

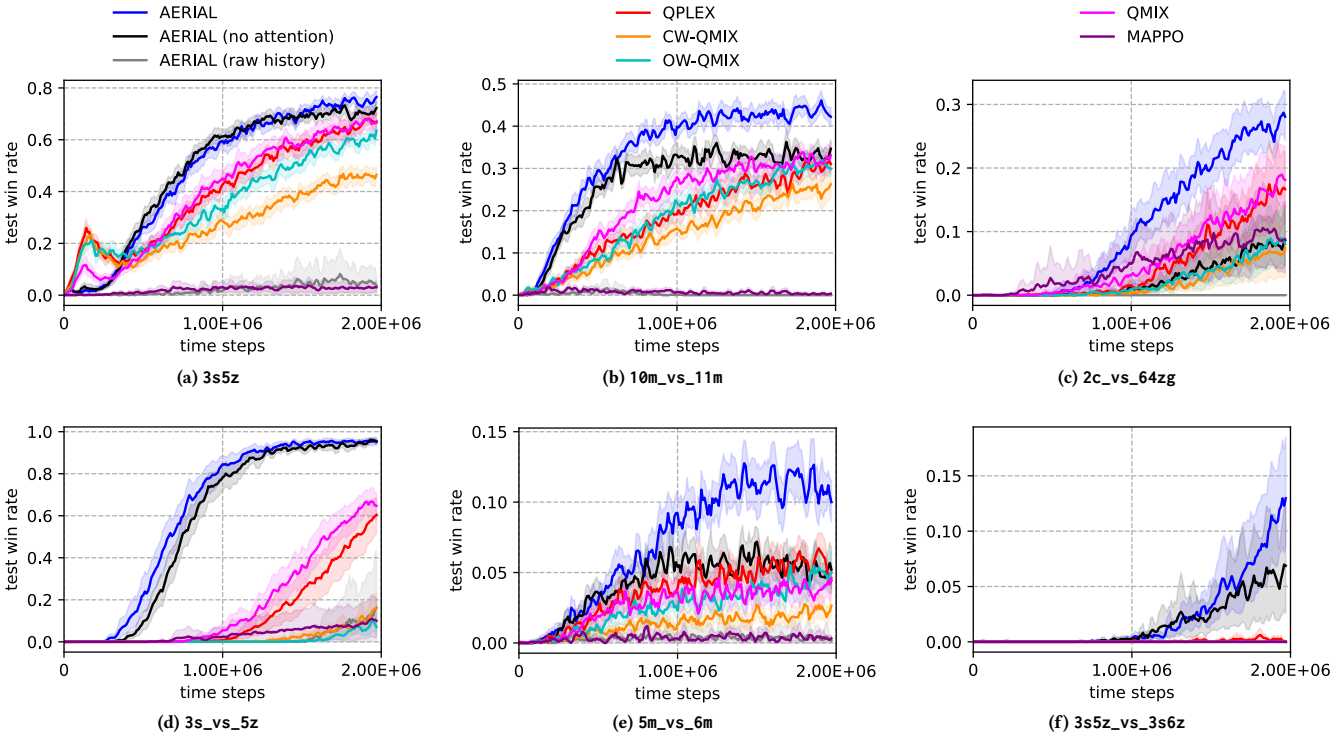

Figure 4: Average learning progress w.r.t. the win rate of AERIAL variants and state-of-the-art baselines in MessySMAC over 20 runs. Shaded areas show the 95% confidence interval. The legend at the top applies across all plots.

Unlike state-based CTDE, AERIAL (no attention) implicitly considers state uncertainty which is more crucial for MessySMAC than for SMAC. However, AERIAL (no attention) naively assumes conditional independence of agent-wise recurrency via $h_{t,i}$ which does not hold in practice thus limiting performance in most maps. Self-attention can correct for the independence assumption as AERIAL consistently outperforms AERIAL (no attention), AERIAL (raw history), and all state-of-the-art baselines. MAPPO performs especially poorly in MessySMAC due to its misleading dependence on true states without any credit assignment mechanism, confirming the findings of [7].

6.4 State Uncertainty Robustness

Setting. We evaluate the robustness of AERIAL and AERIAL (no attention) against various configurations of state uncertainty in MessySMAC by manipulating Ω and b_0 through the observation negation probability ϕ and the number of initial random steps K as defined in Section 4.2 respectively. We compare the results with QMIX and QPLEX as the best performing state-of-the-art baselines in MessySMAC according to the results in Section 6.3. We present summarized plots, where the results are aggregated accross all maps from Section 6.3. To avoid that easy maps dominate the average win rate due to all approaches achieving high values there, we normalize all win rates by the maximum win rate achieved in the respective map for all tested configurations of ϕ and K as explained in the

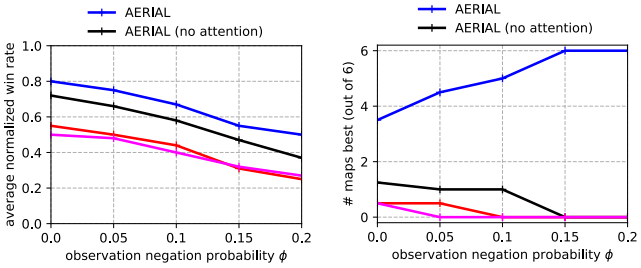

(a) average normalized test win rate (b) # maps best out of 6 scenarios

Figure 5: Evaluation of AERIAL, AERIAL (no attention), and the best MessySMAC baselines for different observation negation probabilities ϕ affecting the stochasticity of the observation function Ω (20 runs per configuration). (a) The average normalized test win rate accross all 6 MessySMAC maps from Section 6.3. (b) The number of maps best out of 6. The legend at the top applies across all plots.

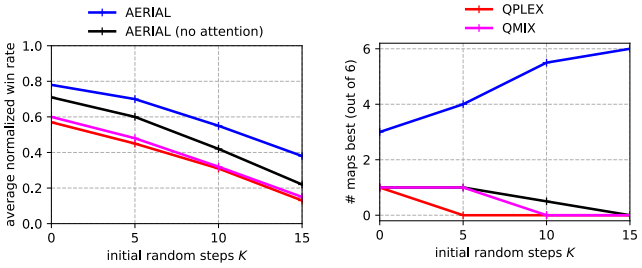

(a) average normalized test win rate (b) # maps best out of 6 scenarios

Figure 6: Evaluation of AERIAL, AERIAL (no attention), and the best MessySMAC baselines for different initial random steps K affecting the stochasticity of the initial state distribution b_0 (20 runs per configuration). (a) The average normalized test win rate accross all 6 MessySMAC maps from Section 6.3. (b) The number of maps best out of 6. The legend at the top applies across all plots.

appendix A.3.3. Thus, we ensure an equal weighting regardless of the particular difficulty level. If not mentioned otherwise, we set $\phi = 15\%$ and $K = 10$ as default parameters based on Section 6.3.

Results. The results regarding stochasticity of the observation function Ω w.r.t. ϕ are shown in Fig. 5. Fig. 5a shows that the average win rates of all approaches decrease with increasing ϕ with AERIAL consistently achieving the highest average win rate in all configurations. Fig. 5b shows that AERIAL performs best in most MessySMAC maps, especially when $\phi \geq 15\%$. AERIAL (no attention) performs second best.

The results regarding stochasticity of the initial state distribution b_0 w.r.t. K are shown in Fig. 6. Analogously to Fig. 5, Fig. 6a shows that the average (normalized) win rates of all approaches decrease with increasing K with AERIAL consistently achieving the highest average win rate in all configurations. Fig. 6b shows that AERIAL performs best in most MessySMAC maps, especially when $K \geq 10$. AERIAL (no attention) performs second best.

Discussion. Our results systematically demonstrate the robustness of AERIAL and AERIAL (no attention) against various configurations of state uncertainty according to Ω and b_0. State-based CTDE is notably less effective in settings, where stochasticity of observations and variance in initial states is high. Since AERIAL consistently performs best in all maps when $\phi \geq 15\%$ or $K \geq 10$, we conclude that exploiting $\mathbf{h_t}$ using self-attention is more beneficial for CTDE than merely relying on true states when facing domains with high degrees of state uncertainty.

7 CONCLUSION AND FUTURE WORK

To tackle multi-agent problems in the real-world that are generally messy and only observable through noisy sensors, we need adequate benchmarks and algorithms considering state uncertainty.

In this paper, we presented *MessySMAC*, a modified version of SMAC with stochastic observations and higher variance in initial states to provide a more general and configurable Dec-POMDP benchmark regarding state uncertainty for systematic evaluation. We demonstrated visually in Fig. 1 and experimentally in Section 6 that MessySMAC scenarios can exhibit higher degrees of state uncertainty than their original counterparts in SMAC thus posing a greater challenge for state-of-the-art MARL.

In addition, we proposed AERIAL to approximate value functions under implicit consideration of state uncertainty by replacing the true state in CTDE with the memory representation of all agents' RNNs, which are processed by a self-attention mechanism.

Compared to state-of-the-art MARL based on state-based CTDE, AERIAL achieves competitive performance in SMAC and superior performance in Dec-Tiger and MessySMAC, which both exhibit higher state uncertainty than SMAC. Simply replacing the true state with memory representations can already improve performance in most scenarios, which confirms the need for state uncertainty consideration in CTDE. Self-attention can correct for the naive independence assumption of agent-wise recurrency by automatically learning the latent dependencies, which further improves performance, especially in domains with high state uncertainty.

Regarding future work, we would like to evaluate AERIAL in other challenging settings like SMACv2 or mixed competitive-cooperative games [7, 18]. Another interesting direction would be the integration of AERIAL in hierarchical factorization schemes for scalable MARL in highly state uncertain environments [24].

REFERENCES

[1] Christopher Amato, Daniel S Bernstein, and Shlomo Zilberstein. 2007. Optimizing Memory-Bounded Controllers for Decentralized POMDPs. In *Proceedings of the 23rd Conference on Uncertainty in Artificial Intelligence*. 1–8.

[2] Daniel S Bernstein, Eric A Hansen, and Shlomo Zilberstein. 2005. Bounded Policy Iteration for Decentralized POMDPs. In *IJCAI*. 52–57.

[3] Craig Boutilier. 1996. Planning, Learning and Coordination in Multiagent Decision Processes. In *Proceedings of the 6th conference on Theoretical aspects of rationality and knowledge*. Morgan Kaufmann Publishers Inc., 195–210.

[4] Lucian Buşoniu, Robert Babuška, and Bart De Schutter. 2010. Multi-Agent Reinforcement Learning: An Overview. In *Innovations in Multi-Agent Systems and Applications-1*. Springer, 183–221.

[5] Lili Chen, Kevin Lu, Aravind Rajeswaran, Kimin Lee, Aditya Grover, Misha Laskin, Pieter Abbeel, Aravind Srinivas, and Igor Mordatch. 2021. Decision Transformer: Reinforcement Learning via Sequence Modeling. In *Advances in Neural Information Processing Systems*, M. Ranzato, A. Beygelzimer, Y. Dauphin,

P.S. Liang, and J. Wortman Vaughan (Eds.), Vol. 34. Curran Associates, Inc., 15084–15097.

[6] Kyunghyun Cho, Bart van Merriënboer, Dzmitry Bahdanau, and Yoshua Bengio. 2014. On the Properties of Neural Machine Translation: Encoder-Decoder Approaches. In *Proceedings of SSST-8, Eighth Workshop on Syntax, Semantics and Structure in Statistical Translation*. 103–111.

[7] Benjamin Ellis, Skander Moalla, Mikayel Samvelyan, Mingfei Sun, Anuj Mahajan, Jakob N. Foerster, and Shimon Whiteson. 2022. SMACv2: An Improved Benchmark for Cooperative Multi-Agent Reinforcement Learning. https://arxiv.org/abs/2212.07489

[8] Rosemary Emery-Montemerlo, Geoff Gordon, Jeff Schneider, and Sebastian Thrun. 2004. Approximate Solutions for Partially Observable Stochastic Games with Common Payoffs. In *Proceedings of the Third International Joint Conference on Autonomous Agents and Multiagent Systems - Volume 1* (New York, New York) *(AAMAS '04)*. IEEE Computer Society, USA, 136–143.

[9] Jakob Foerster, Gregory Farquhar, Triantafyllos Afouras, Nantas Nardelli, and Shimon Whiteson. 2018. Counterfactual Multi-Agent Policy Gradients. *Proceedings of the AAAI Conference on Artificial Intelligence* 32, 1 (Apr. 2018).

[10] Jayesh K Gupta, Maxim Egorov, and Mykel Kochenderfer. 2017. Cooperative Multi-Agent Control using Deep Reinforcement Learning. In *Autonomous Agents and Multiagent Systems*. Springer, 66–83.

[11] Matthew Hausknecht and Peter Stone. 2015. Deep Recurrent Q-Learning for Partially Observable MDPs. In *2015 AAAI Fall Symposium Series*.

[12] Sepp Hochreiter and Jürgen Schmidhuber. 1997. Long Short-Term Memory. *Neural Computation* 9, 8 (1997), 1735–1780.

[13] Hengyuan Hu and Jakob N Foerster. 2019. Simplified Action Decoder for Deep Multi-Agent Reinforcement Learning. In *ICLR 2019*.

[14] Shariq Iqbal, Christian A Schroeder De Witt, Bei Peng, Wendelin Boehmer, Shimon Whiteson, and Fei Sha. 2021. Randomized Entity-wise Factorization for Multi-Agent Reinforcement Learning. In *Proceedings of the 38th International Conference on Machine Learning (Proceedings of Machine Learning Research, Vol. 139)*, Marina Meila and Tong Zhang (Eds.). PMLR, 4596–4606.

[15] Shariq Iqbal and Fei Sha. 2019. Actor-Attention-Critic for Multi-Agent Reinforcement Learning. In *Proceedings of the 36th International Conference on Machine Learning (Proceedings of Machine Learning Research, Vol. 97)*, Kamalika Chaudhuri and Ruslan Salakhutdinov (Eds.). PMLR, Long Beach, California, USA, 2961–2970.

[16] Leslie Pack Kaelbling, Michael L Littman, and Anthony R Cassandra. 1998. Planning and Acting in Partially Observable Stochastic Domains. *Artificial intelligence* 101, 1-2 (1998), 99–134.

[17] Kaixiang Lin, Renyu Zhao, Zhe Xu, and Jiayu Zhou. 2018. Efficient Large-Scale Fleet Management via Multi-Agent Deep Reinforcement Learning. In *Proceedings of the 24th ACM SIGKDD International Conference on Knowledge Discovery & Data Mining* (London, United Kingdom) *(KDD '18)*. Association for Computing Machinery, New York, NY, USA, 1774–1783. https://doi.org/10.1145/3219819.3219993

[18] Ryan Lowe, Yi Wu, Aviv Tamar, Jean Harb, Pieter Abbeel, and Igor Mordatch. 2017. Multi-Agent Actor-Critic for Mixed Cooperative-Competitive Environments. In *Advances in Neural Information Processing Systems*, I. Guyon, U. V. Luxburg, S. Bengio, H. Wallach, R. Fergus, S. Vishwanathan, and R. Garnett (Eds.), Vol. 30. Curran Associates, Inc.

[19] Xueguang Lyu, Andrea Baisero, Yuchen Xiao, and Christopher Amato. 2022. A Deeper Understanding of State-Based Critics in Multi-Agent Reinforcement Learning. *Proceedings of the AAAI Conference on Artificial Intelligence* 36, 9 (Jun. 2022), 9396–9404. https://doi.org/10.1609/aaai.v36i9.21171

[20] Xueguang Lyu, Yuchen Xiao, Brett Daley, and Christopher Amato. 2021. Contrasting Centralized and Decentralized Critics in Multi-Agent Reinforcement Learning. In *Proceedings of the 20th International Conference on Autonomous Agents and Multiagent Systems*. 844–852.

[21] R. Nair, M. Tambe, M. Yokoo, D. Pynadath, and S. Marsella. 2003. Taming Decentralized POMDPs: Towards Efficient Policy Computation for Multiagent Settings. In *Proceedings of the 18th International Joint Conference on Artificial Intelligence* (Acapulco, Mexico) *(IJCAI'03)*. Morgan Kaufmann Publishers Inc., San Francisco, CA, USA, 705–711.

[22] Frans A Oliehoek and Christopher Amato. 2016. *A Concise Introduction to Decentralized POMDPs*. Vol. 1. Springer.

[23] Frans A Oliehoek, Matthijs TJ Spaan, and Nikos Vlassis. 2008. Optimal and Approximate Q-Value Functions for Decentralized POMDPs. *Journal of Artificial Intelligence Research* 32 (2008), 289–353.

[24] Thomy Phan, Fabian Ritz, Lenz Belzner, Philipp Altmann, Thomas Gabor, and Claudia Linnhoff-Popien. 2021. VAST: Value Function Factorization with Variable Agent Sub-Teams. In *Advances in Neural Information Processing Systems*, M. Ranzato, A. Beygelzimer, Y. Dauphin, P.S. Liang, and J. Wortman Vaughan (Eds.), Vol. 34. Curran Associates, Inc., 24018–24032.

[25] Tabish Rashid, Gregory Farquhar, Bei Peng, and Shimon Whiteson. 2020. Weighted QMIX: Expanding Monotonic Value Function Factorisation for Deep Multi-Agent Reinforcement Learning. In *Advances in Neural Information Processing Systems*, H. Larochelle, M. Ranzato, R. Hadsell, M. F. Balcan, and H. Lin (Eds.), Vol. 33. Curran Associates, Inc., 10199–10210.

[26] Tabish Rashid, Mikayel Samvelyan, Christian Schroeder De Witt, Gregory Farquhar, Jakob Foerster, and Shimon Whiteson. 2020. Monotonic Value Function Factorisation for Deep Multi-Agent Reinforcement Learning. *The Journal of Machine Learning Research* 21, 1 (2020), 7234–7284.

[27] Tabish Rashid, Mikayel Samvelyan, Christian Schroeder, Gregory Farquhar, Jakob Foerster, and Shimon Whiteson. 2018. QMIX: Monotonic Value Function Factorisation for Deep Multi-Agent Reinforcement Learning. In *Proceedings of the 35th International Conference on Machine Learning (Proceedings of Machine Learning Research, Vol. 80)*, Jennifer Dy and Andreas Krause (Eds.). PMLR, 4295–4304.

[28] Mikayel Samvelyan, Tabish Rashid, Christian Schroeder de Witt, Gregory Farquhar, Nantas Nardelli, Tim GJ Rudner, Chia-Man Hung, Philip HS Torr, Jakob Foerster, and Shimon Whiteson. 2019. The StarCraft Multi-Agent Challenge. In *Proceedings of the 18th International Conference on Autonomous Agents and Multiagent Systems* (Montreal QC, Canada) *(AAMAS '19)*. International Foundation for Autonomous Agents and Multiagent Systems, Richland, SC, 2186–2188.

[29] Kyunghwan Son, Daewoo Kim, Wan Ju Kang, David Earl Hostallero, and Yung Yi. 2019. QTRAN: Learning to Factorize with Transformation for Cooperative Multi-Agent Reinforcement Learning. In *Proceedings of the 36th International Conference on Machine Learning (Proceedings of Machine Learning Research, Vol. 97)*, Kamalika Chaudhuri and Ruslan Salakhutdinov (Eds.). PMLR, 5887–5896.

[30] Peter Sunehag, Guy Lever, Audrunas Gruslys, Wojciech Marian Czarnecki, Vinicius Zambaldi, Max Jaderberg, Marc Lanctot, Nicolas Sonnerat, Joel Z. Leibo, Karl Tuyls, and Thore Graepel. 2018. Value-Decomposition Networks for Cooperative Multi-Agent Learning based on Team Reward. In *Proceedings of the 17th International Conference on Autonomous Agents and Multiagent Systems* (Stockholm, Sweden) *(AAMAS '18)*. International Foundation for Autonomous Agents and Multiagent Systems, Richland, SC, 2085–2087.

[31] Daniel Szer, François Charpillet, and Shlomo Zilberstein. 2005. MAA*: A Heuristic Search Algorithm for Solving Decentralized POMDPs *(UAI'05)*. AUAI Press, Arlington, Virginia, USA, 576–583.

[32] Ming Tan. 1993. Multi-Agent Reinforcement Learning: Independent versus Cooperative Agents. In *Proceedings of the Tenth International Conference on International Conference on Machine Learning* (Amherst, MA, USA) *(ICML'93)*. Morgan Kaufmann Publishers Inc., San Francisco, CA, USA, 330–337.

[33] Ashish Vaswani, Noam Shazeer, Niki Parmar, Jakob Uszkoreit, Llion Jones, Aidan N Gomez, Ł ukasz Kaiser, and Illia Polosukhin. 2017. Attention is All You Need. In *Advances in Neural Information Processing Systems*, I. Guyon, U. V. Luxburg, S. Bengio, H. Wallach, R. Fergus, S. Vishwanathan, and R. Garnett (Eds.), Vol. 30. Curran Associates, Inc.

[34] Oriol Vinyals, Igor Babuschkin, Wojciech M Czarnecki, Michaël Mathieu, Andrew Dudzik, Junyoung Chung, David H Choi, Richard Powell, Timo Ewalds, Petko Georgiev, et al. 2019. Grandmaster Level in StarCraft II using Multi-Agent Reinforcement Learning. *Nature* (2019), 1–5.

[35] Jianhao Wang, Zhizhou Ren, Terry Liu, Yang Yu, and Chongjie Zhang. 2021. QPLEX: Duplex Dueling Multi-Agent Q-Learning. In *International Conference on Learning Representations*.

[36] Christopher JCH Watkins and Peter Dayan. 1992. Q-Learning. *Machine Learning* 8, 3-4 (1992), 279–292.

[37] Muning Wen, Jakub Grudzien Kuba, Runji Lin, Weinan Zhang, Ying Wen, Jun Wang, and Yaodong Yang. 2022. Multi-Agent Reinforcement Learning is a Sequence Modeling Problem. *arXiv preprint arXiv:2205.14953* (2022).

[38] Yaodong Yang, Jianye Hao, Ben Liao, Kun Shao, Guangyong Chen, Wulong Liu, and Hongyao Tang. 2020. Qatten: A General Framework for Cooperative Multiagent Reinforcement Learning. *arXiv preprint arXiv:2002.03939* (2020).

[39] Chao Yu, Akash Velu, Eugene Vinitsky, Jiaxuan Gao, Yu Wang, Alexandre Bayen, and Yi Wu. 2022. The Surprising Effectiveness of PPO in Cooperative Multi-Agent Games. In *36th Conference on Neural Information Processing Systems Datasets and Benchmarks Track*.

A APPENDIX

A.1 Dec-Tiger Example

Given the Dec-Tiger example (Section 5.1) with a horizon of $T = 2$, the tiger being behind the right door (s_R), and both agents having listened in the first step, where agent 1 heard z_L and agent 2 heard z_R: The final state-based values are defined by $Q^*_{MDP}(s_t, \mathbf{a_t}) = \mathcal{R}(s_t, \mathbf{a_t})$.

Due to both agents perceiving different observations, i.e., z_L and z_R respectively, the probability of being in state s_R is 50% according to the belief state, i.e., $b(s_R|\boldsymbol{\tau_t}) = b(s_L|\boldsymbol{\tau_t}) = \frac{1}{2}$. Thus, the true optimal Dec-POMDP values for the final time step are defined by:

$$\begin{aligned} Q^*(\boldsymbol{\tau_t}, \mathbf{a_t}) &= \sum_{s_t \in \mathcal{S}} b(s_t|\boldsymbol{\tau_t}) \mathcal{R}(s_t, \mathbf{a_t}) \\ &= \frac{1}{2}(Q^*_{MDP}(s_L, \mathbf{a_t}) + Q^*_{MDP}(s_R, \mathbf{a_t})) \end{aligned} \tag{10}$$

The values of Q^*_{MDP} and Q^* for the final time step $t = 2$ in the example are given in Table 2. Both agents can reduce the expected penalty when always performing the same action. Therefore, it is likely for MARL to converge to a joint policy that recommends the same actions for both agents, especially when synchronization techniques like parameter sharing are used [10, 32, 39].

Table 2: The values of Q^*_{MDP} and Q^* for the final time step $t = 2$ in the Dec-Tiger example from Section 5.1.

$\mathbf{a_t}$	$Q^*_{MDP}(s_L, \mathbf{a_t})$	$Q^*_{MDP}(s_R, \mathbf{a_t})$	$Q^*(\boldsymbol{\tau_t}, \mathbf{a_t})$
$\langle li, li \rangle$	−2	−2	−2
$\langle li, o_L \rangle$	-101	+9	-46
$\langle li, o_R \rangle$	+9	-101	-46
$\langle o_L, li \rangle$	-101	+9	-46
$\langle \mathbf{o_L}, \mathbf{o_L} \rangle$	**−50**	**+20**	**−15**
$\langle o_L, o_R \rangle$	-100	-100	-100
$\langle o_R, li \rangle$	+9	-101	-46
$\langle o_R, o_L \rangle$	-100	-100	-100
$\langle \mathbf{o_R}, \mathbf{o_R} \rangle$	**+20**	**−50**	**−15**

A.2 Full Algorithm of AERIAL

The complete formulation of AERIAL is given in Algorithm 1. Note that AERIAL does not depend on true states s_t at all, since the experience samples e_t (Line 20) used for training do not record any states.

Algorithm 1 AERIAL

1: Initialize parameters for $\langle Q_i \rangle_{i \in \mathcal{D}}$ and Ψ.
2: **for** episode $m \leftarrow 1, E$ **do**
3: Sample s_0, $\mathbf{z_0}$, and $\boldsymbol{\tau_0}$ via b_0 and Ω
4: **for** time step $t \leftarrow 0, T-1$ **do**
5: **for** agent $i \in \mathcal{D}$ **do**
6: $a_{t,i} \leftarrow \pi_i(\tau_{t,i})$ ▷ $argmax_{a_{t,i} \in \mathcal{A}_i} Q_i(\tau_{t,i}, a_{t,i})$
7: $rand \sim U(0, 1)$ ▷ Sample from uniform distribution
8: **if** $rand \leq \epsilon$ **then** ▷ ϵ-greedy exploration
9: Select random action $a_{t,i} \in \mathcal{A}_i$
10: $\mathbf{a_t} \leftarrow \langle a_{t,i} \rangle_{i \in \mathcal{D}}$
11: Execute joint action $\mathbf{a_t}$
12: $s_{t+1} \sim \mathcal{T}(s_{t+1}|s_t, \mathbf{a_t})$
13: $\mathbf{z_{t+1}} \sim \Omega(\mathbf{z_{t+1}}|\mathbf{a_t}, s_{t+1})$
14: $\mathbf{h_t} \leftarrow \langle h_{t,i} \rangle_{i \in \mathcal{D}}$ ▷ Query all memory representations
15: Detach $\mathbf{h_t}$ from computation graph
16: $\boldsymbol{\tau_{t+1}} \leftarrow \langle \boldsymbol{\tau_t}, \mathbf{a_t}, \mathbf{z_{t+1}} \rangle$ ▷ Concatenate $\boldsymbol{\tau_t}$, $\mathbf{a_t}$, and $\mathbf{z_{t+1}}$
17: **for** attention head $c \leftarrow 1, C$ **do** ▷ Process multi-agent recurrency
18: $attention_c \leftarrow att_c(\mathbf{h_t})$ ▷ See Eq. 9
19: $rec_t \leftarrow MLP(\sum_{c=1}^{C} attention_c)$ ▷ See Section 5.2
20: $e_t \leftarrow \langle \boldsymbol{\tau_t}, \mathbf{a_t}, r_t, \mathbf{z_{t+1}}, rec_t \rangle$
21: Store experience sample e_t
22: Train Ψ and $\langle Q_i \rangle_{i \in \mathcal{D}}$ using all e_t ▷ See Fig. 2

A.3 Experiment Details

A.3.1 ***Computing infrastructure.*** All training and test runs were performed in parallel on a computing cluster of fifteen x86_64 GNU/Linux (Ubuntu 18.04.5 LTS) machines with i7-8700 @ 3.2GHz CPU (8 cores) and 64 GB RAM. We did not use any GPU in our experiments.

A.3.2 ***Hyperparameters and Neural Network Architectures.*** Our experiments are based on PyMARL and the code from [25]. We used the default setting from the paper without further hyperparameter tuning as well as the same neural network architectures for the RNNs and the respective factorization operators Ψ as specified by default for each state-of-the-art baseline in Section 6. For `MAPPO`, we used the hyperparameters suggested in [39] for SMAC.

`AERIAL` is implemented using `QMIX` as factorization operator Ψ according to Fig. 2. We also experimented with `QPLEX` as alternative with no significant difference in performance. Thus, we stick with `QMIX` for computational efficiency due to less trainable parameters. The transformer has $C = 4$ heads with MLPs W_q, W_k, and W_v, each having one hidden layer of $d_{att} = 64$ units with ReLU activation. The three subsequent MLP layers have 64 units with ReLU activation.

A.3.3 ***Aggregated Measures.*** In Fig. 5 and 6, we provide aggregated results accross all maps from Section 6.3 with $\phi = 15\%$ and $K = 10$ as default parameters. We define $\theta = \langle \phi, K \rangle$ as *(state uncertainty) configuration* for any map ξ from Section 6.3.

Since all approaches achieve high win rates $w_{\xi,\theta}$ in easy maps, the naive average win rate would be dominated by the performance of all approaches in easy maps. Thus, we report the average of *normalized win rates* $\overline{w}_{\xi,\theta}$ in Fig. 5a and 6a to ensure an equal weighting regardless of the actual difficulty level:

$$\overline{w}_{\xi,\theta} = \frac{w_{\xi,\theta}}{max_{\theta'} w_{\xi,\theta'}} \tag{11}$$

where $max_{\theta'} w_{\xi,\theta'}$ is the maximum win rate achieved by the respective best approach in map ξ for all tested configurations θ'.

The "number of maps best out of 6"-measure used in Fig. 5b and 6b counts the number of maps for each approach, where the highest win rate $w_{\xi,\theta}$ compared to all other approaches has been achieved for 20 runs per configuration θ.